Housing & Building National Research Center

Seventh International Conference on NANO-TECHNOLOGY IN CONSTRUCTION
المؤتمر الدولي السابع لتكنولوجيا النانو في الإنشاء
(NTC 2014)

Egyptian-Russian University

Izhevsk State Technical University (ISTU)

Modeling Mechanical Behavior of Open-Hole Plain-Woven Composite Laminates under Tensile Loading

Abdalla M. A. Ahmed[1,*] & [1] Mohamed N. A. Nasr[2]

[1]Dept. of Materials Science & Engineering, Egypt-Japan University of Science & Technology, EGYPT
[2]Dept. of Mechanical Engineering, Faculty of Engineering, Alexandria University, EGYPT

Abstract In the current work, finite element modelling has been used to predict progressive failure of open-hole woven glass fiber-reinforced polyester composite laminates, under tensile loading. This has been done with the aid of multicontinuum theory, in order to extract constituents' stress and strain components. The model was first validated using previously published experimental results for open-hole composite laminates. After that, the effects of fiber orientation on the laminate mechanical behavior have been examined by modelling two cases; cross-ply and angle-ply laminates. In addition, a model without a central hole has been built for both fiber orientations, in order to evaluate the effects of the central hole on overall stiffness and load carrying capacity. The results were explained in terms of local stress state, and agreed with previously published experimental results.

Keywords Woven, GFRP, Orientation, FEM, Open-hole, Progressive failure

1 Introduction

Fiber-reinforced polymer (FRP) woven composites are being currently used for numerous applications, especially in the aerospace and automobile sectors. This is mainly attributed to their high strength-to-weight ratio. The mechanical properties of woven composites mainly depend on the fiber volume fraction, mechanical properties of fibers, matrix and interface, and the weaving parameters (size, spacing, and undulation of strands) [1]. Different approaches have been tried in order to determine the mechanical properties of woven composites based on those of their constituents; however, no general theory has been identified yet. In general, woven composites are analyzed, according to the laminate theory, as an equivalent stack of unidirectional angle-plied lamina, where the undulation effect is neglected [2,3]. Alternatively, different analytical methods have been established that take into consideration the undulation geometry, as a sinusoidal or circular strand, in order to predict the overall composite mechanical properties [4–8]. Finite element modelling (FEM) has been also used in order to simulate the undulation effects, where a detailed geometry with two undulated plies is modelled, in an effort to predict the elastic properties of woven composites [9–11]. Chun et al. [12] experimentally studied the impact of undulations on the elastic properties of carbon/epoxy composites, under tensile loading. They fabricated unidirectional plates with different undulation-to-fiber period ratios; i.e., cases with higher undulation-to-fiber period ratios represent more serious undulation effects. It was found that, samples with higher undulation ratios showed significantly lower elastic moduli. At the same time, the sample stiffness experienced progressive increase with increasing load; this was basically attributed to the stretching effect of undulations.

As part of the mechanical characterization of composite laminate joints, the open-hole (O-Hole) tensile test (OHTT) is used to determine their mechanical strength. The O-Hole tensile (OHT) strength is an important parameter that limits the load carrying capability and controls the damage mechanics of those laminates, especially for riveted and bolted joints [13]. The damage and fracture mechanisms of composite laminates containing holes are highly confounded due to the stress concentration effects, as well as the interaction between various stress components. Since glass fiber-reinforced polymer composite laminates are widely used in several applications, several analytical, numerical and experimental works were carried out in order to determine their OHT strength. As an example, Belmonte et al. [14] studied the fracture and damage growth at circular holes in woven E-glass/epoxy composite laminates, with different fiber orientation, under tensile loading, both experimentally and analytically. They found that the notch-edge damage initiation and propagation comprised matrix cracking, fracture of the 0º tows, delamination and longitudinal splitting. However, the tows in the fabric layers oriented at 45º within the damage zone remained intact up to the maximum load in a tensile test. O'Higgins et al. [15] experimentally compared the OHT strength of carbon versus glass fiber-reinforced polymers. It was found out that, the

*e-mail: abdalla.ahmed@ejust.edu.eg

glass fiber samples experienced lower levels of matrix cracking in the 90º plies compared to the carbon fiber ones.

In the present work, FEM has been used to model the effects of fiber orientation on the mechanical behavior of O-Hole plain woven glass fiber-reinforced polyester (GFRP) laminates under tensile loading. Two woven fiber orientations were used; 0º and 45º. In addition, the effects of including a central hole were evaluated by comparing the mechanical behavior of O-Hole samples to samples without central hole (W/O-Hole). The commercial finite element software ABAQUS/Standard V6.12 was used, and a commercial plug-in by Autodesk "Autodesk Simulation Composite Analysis" was employed to efficiently model progressive failure. The Multi-Continuum Theory (MCT), based on the approach developed by Key et al. [16], was used in order to extract average individual constituent (fibers and matrix) stresses and strains from composite stresses and strains. The model was validated using previously published experimental results by Shindo et al. [17], for O-Hole 0º samples under tensile loading.

2 Finite Element Model

2.1 Model Description

The commercial finite element software ABAQUS/Standard V6.12 was used in the current study, along with the Autodesk Simulation Composite Analysis (ASCA) material manager to define and handle material properties, as explained below. The MCT approach was used to extract average individual constituent (fibers and matrix) stresses and strains from the composite stresses and strains. Stress-based failure criterion with instantaneous material property degradation, and displacement-controlled loading were used in all cases. Since no experimental results were available for O-Hole woven GFRP laminates, current interest, the current model was validated using the experimental results by Shindo et al. [17] for woven-glass fiber reinforced epoxy. Accordingly, two sets of O-Hole models were built; Model-1 for experimental validation and Model-2 for examining the effects of fiber orientation and central hole on mechanical behavior.

In all models, a static, general step was used. Output state variables (SDVs), available in Abaqus, were requested in order to track constituents progressive failure. Only SDV1, which is a discrete damage state variable that assigns a finite number of discrete values between 1 and 3 to represent different modes of failure, is presented in the current paper.

2.1.1 Model-1 (Experimental Validation)

To the authors' best of knowledge, the only available experimental results for woven O-Hole composite laminates are those presented by Shindo et al. [17], for 0º glass/epoxy laminates. Accordingly, Model-1 was built similar to the experimental setup presented in [17] for validation purposes. Sample geometry is similar to that of Fig. 1 with the following dimensions: 120 x 25 x 2 mm and 4.2 mm diameter central hole. The laminate consists of 12-plain woven plies of equal thicknesses, with fiber volume fraction (V_f) of 47%, and the material properties as shown in Table 1 and Table 2. Boundary conditions and loading are similar to those in Fig. 1. The constituent materials properties were optimized using the ASCA material manager.

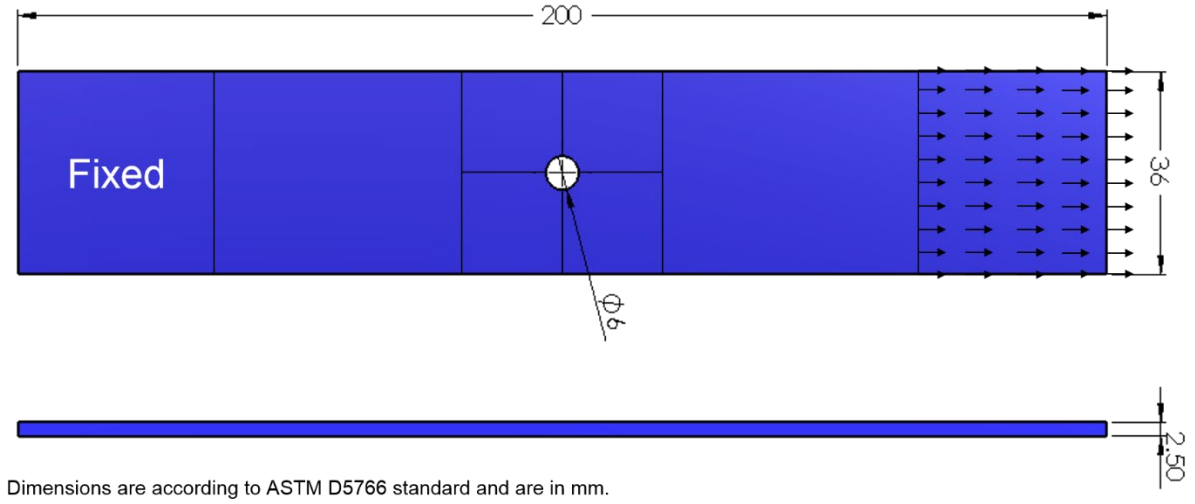

Fig. 1 Open-hole model (ASTM D-5766)

Table 1. Model-1 composite material elastic properties

	E_{11} (GPa)	E_{22} (GPa)	E_{33} (GPa)	G_{12} (GPa)	G_{13} (GPa)	G_{23} (GPa)	ν_{12}	ν_{13}	ν_{23}
Experimental	27.9	24.1	-	6.2	-	-	0.170	-	-
Modelling	27.9	27.9	11.6	5.9	3.6	3.6	0.133	0.307	0.307

Table 2. Model-1 composite material failure stresses

	$^{+}\sigma_{11}$ (MPa)	$^{-}\sigma_{11}$ (MPa)	σ_{12} (MPa)
Experimental	325	-332	108
Modelling	325	-332	108

2.1.2 Model-2

This model was built as per ASTM D-5766 in order to examine the effects of fiber orientation, as well as the existence of a central hole, on the mechanical behavior of plain woven GFRP. Figure 1 shows the sample dimensions, boundary conditions and loading. The sample thickness is 2.5 mm, and the width-to-hole diameter ratio and the diameter-to-thickness ratio are 6 and 2.4, respectively. Two fiber orientations were used, 0º and 45º, in order to examine the effect of fiber orientation. In order to evaluate the effect of having a central hole, a model W/O-Hole was also built. The sample W/O-Hole model has exactly the same dimensions as Model-2, except for the hole. The fiber volume fraction (V_f) is 50% for all cases; this was based on experimental trials and previously published data [18]. It is important to note that, ASTM D-5766 does not specify the number of plies. In the current work, 4-plies laminates were modelled based on experimental trials and data available in the literature.

The Autodesk Composite Material Manager was used to determine the mechanical properties of woven GFRP laminates from those of unidirectional laminates. The constituents material properties were obtained from [19] and [20] for E-glass fibers and polyester resin, respectively. Model-2 material properties are presented in Table 3 and Table 4.

Table 3. Model-2 material elastic properties

	E_{11} (GPa)	E_{22} (GPa)	E_{33} (GPa)	G_{12} (GPa)	G_{13} (GPa)	G_{23} (GPa)	ν_{12}	ν_{13}	ν_{23}
Unidirectional	37.6	9.2	9.2	3.2	3.2	3.1	0.282	0.282	0.474
Woven	23.1	23.1	23.1	3.3	2.6	2.6	0.109	0.368	0.368

Table 4. Model-2 material failure stresses

(MPa)	$^{+}\sigma_{11}$	$^{-}\sigma_{11}$	σ_{12}	$^{+}\sigma_{22}$	$^{-}\sigma_{22}$	σ_{13}	$^{+}\sigma_{33}$	$^{-}\sigma_{33}$	σ_{23}
Unidirectional	1075	-725	118	58	-283	118	57	-285	94
Woven	134	-455	47	-	-	-	-	-	-

2.1.3 Mesh Description

Three dimensional eight-node brick continuum elements, with reduced integration (C3D8R) were used in all cases. The model was partitioned, and a refined mesh was used around the central hole in order to capture steep stress gradients. Figure 2 shows a zoomed-in view of the used mesh around the hole.

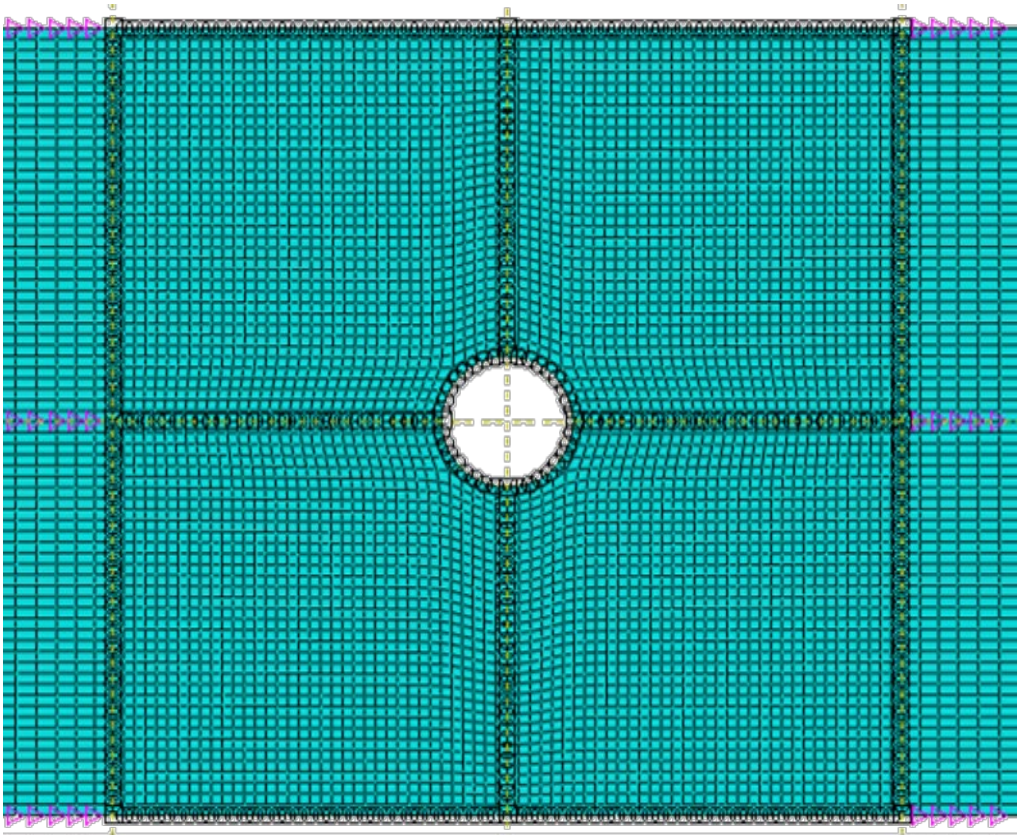

Fig. 2 Open-hole model mesh

2.1.4 Multicontinuum Theory (MCT)

Conventional modelling methods treat composite lamina as homogeneous solids with uniform properties [21]. The MCT approach incorporates the classical micromechanics-based strain decomposition technique of Hill [22] in a numerical algorithm, which allows volume average constituent (fiber and matrix) stresses to be extracted from homogenized composite stresses. It treats the constituents as independent, yet connected, continua and determines their responses at each point in the structure so that failure of every constituent can be assessed [23]. Key et al. [16] used the MCT approach to analyze woven fabric composites into three separate but linked continua; the warp bundles, fill bundles, and pure matrix pockets. Also, they developed two progressive failure models for the analysis of plain woven composite materials [24]. They used constituent phase averaged stress fields in conjunction with a stress based and damage based failure criterion, in order to construct a nonlinear progressive failure algorithm for the woven fabric composite material. When failure is detected, the elastic properties of the failed constituent are degraded and, correspondingly, the composite elastic properties are appropriately degraded [25]. It is important to note that, the fiber stiffness is instantly reduced to a small amount of sample W/O-Hole stiffness. More details about the MCT could be found in [16,21–25].

3 Results and Discussion

3.1 Model Validation

Two critical parameters in controlling failure of composite materials when using MCT are the matrix post failure degradation (MPFD) and fiber post failure degradation (FPFD) parameters. The post failure degradation parameter represents the magnitude of elastic moduli – of the corresponding constituent – after failure as a fraction of their initial values; i.e., it represents the residual stiffness after failure. As an example, a value of 0.1 means that the damaged component retains only 10% of its original undamaged stiffness. The degradation values depend on the composite type (woven or unidirectional), fiber/matrix combination, as well as loading conditions [26]. Since when a fiber fails it completely losses its ability to support loads, a typical value for FPFD is 0.01. On the other hand, polymer matrices typically fail by micro-cracking; accordingly, the matrix does not totally lose its stiffness after failure. Therefore, different MPFD values have been used in the literature [26]. In order to choose a representative MPFD value for the current case, different values were tried. Figure 3 presents the tensile stress-strain curves for two cases; MPFD of 0.1 and 0.7; FPFD was 0.01 in all cases.

As can be seen, the magnitude of MPFD has no effect on the mechanical behavior before the first evidence of failure. In addition, cases with higher MPFD values retain higher fraction of their initial stiffness after failure. These simple, and

expected, results show that the basics of the current model work fine. Comparing the current stress-strain curves to the experimental one shows that the case with MPFD of 0.7 closely predicts the mechanical behavior of the case under investigation. The FE stress-strain curve predicts almost the same experimental failure stress (200 MPa); however, it over predicts strain. In other words, it under predicts stress by about 20 MPa (less than 10% of failure stress) for the same applied strain. Therefore, the current model is capable of capturing the mechanical behavior of plain-woven FRP O-Hole laminates under tensile loading. After proving the validity of the current model, the same procedure was used to; 1) examine the effects of fiber orientation on the mechanical behavior of woven O-Hole FRP laminates; and, 2) evaluate the effects of having a central hole in these laminates (by comparing them to sample W/O-Hole).

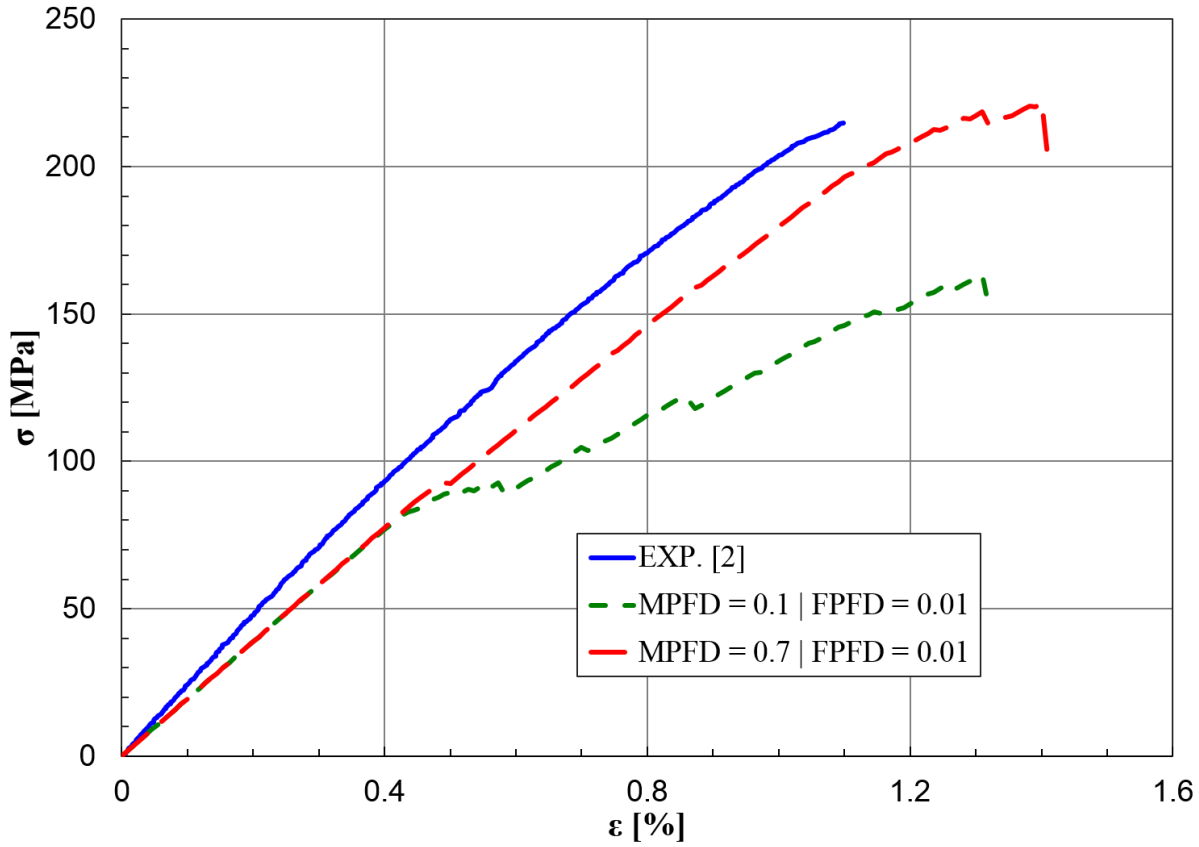

Fig. 3 Model-1 stress-strain curves vs. experimental results (model validation)

3.2 Model-2 Global Failure Analysis

As mentioned earlier, after proving the validity of the current model using Model-1, Model-2 was built in order to examine the effects of fiber orientation on the mechanical behavior of plain-woven O-Hole GFRP laminates under tensile loading. Since this portion of the work is basically a relative evaluation rather than a quantitative failure analysis, the ASCA MPFD default value (0.1) was used here. Figure 4 presents the load/displacement response of the 0º and 45º O-Hole as well as sample W/O-Hole GFRP laminates. From the figure, a detailed comparison could be made between different cases with regards to load carrying capacity (F_{max}) and initial stiffness (before failure onset). Figures 5 and 6 present these comparisons, respectively, in detail.

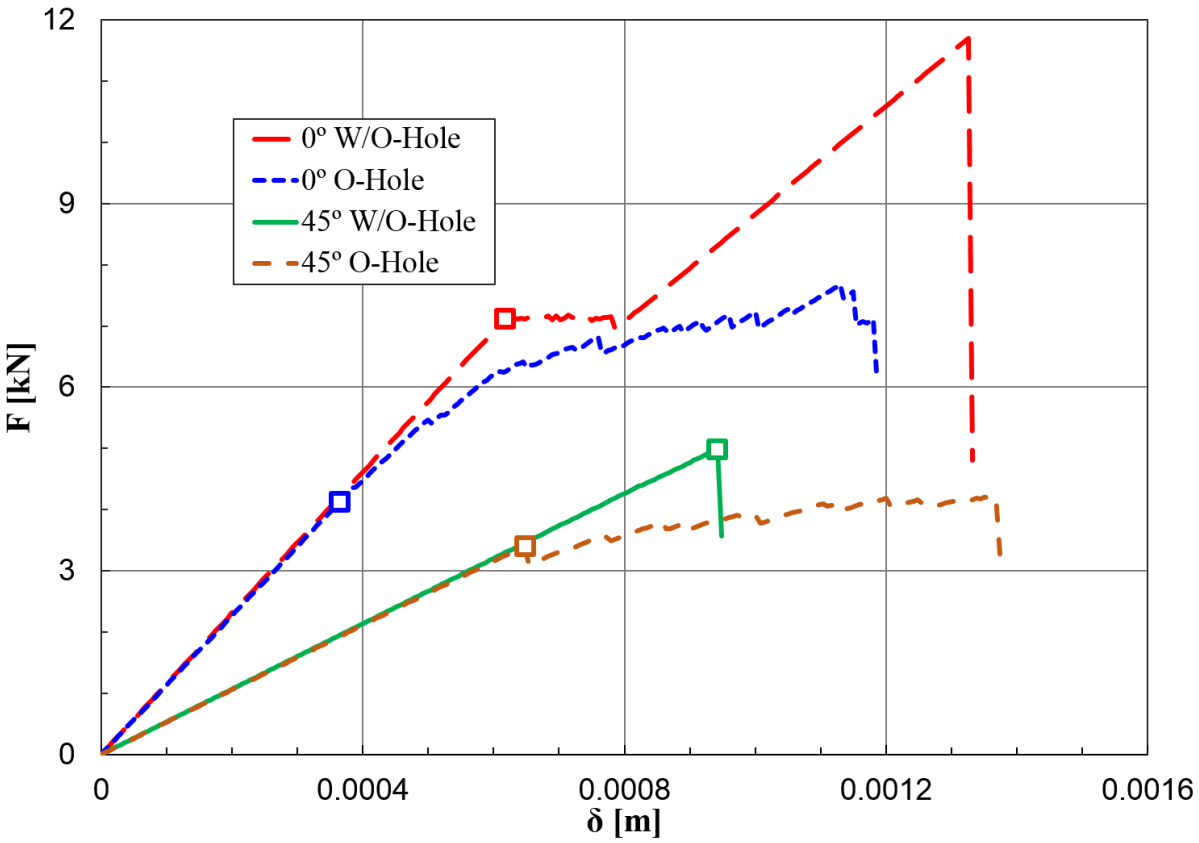

Fig. 4 Load-displacement curve of open-hole and sample without hole models

Figure 5 compares the load carrying capacity (F_{max}) of different laminates. As can be seen, the 0º laminates – both O-Hole and sample W/O-Hole – have higher failure loads compared to the 45º laminates.

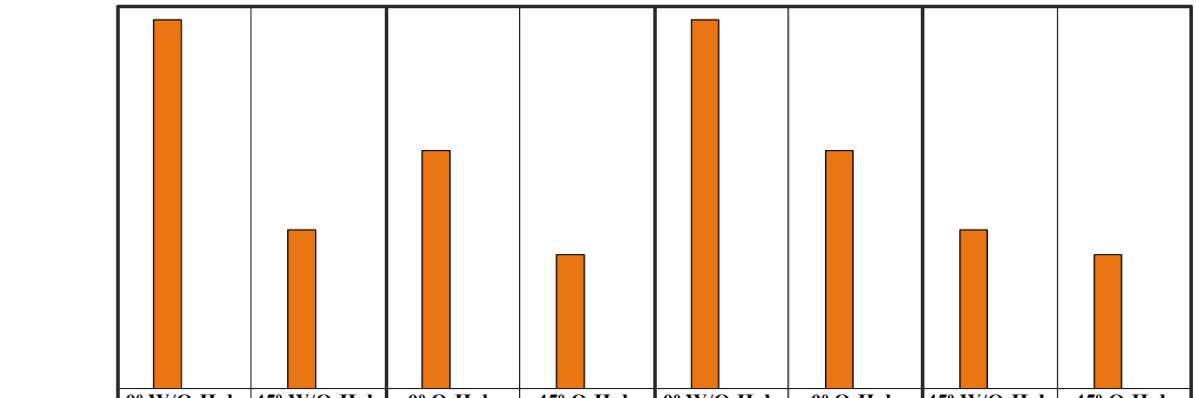

	0º W/O-Hole	45º W/O-Hole	0º O-Hole	45º O-Hole	0º W/O-Hole	0º O-Hole	45º W/O-Hole	45º O-Hole
Fmax [N]	11600	4987	7494	4212	11600	7494	4987	4212
Ratios	2.3	1	1.8	1	1.6	1	1.2	1

Fig. 5 Load carrying capacity (F_{max}) of different laminates

Using simple stress transformation relations (Equation 1), the local stress components for both cases are as follows: for 0º laminates; $\sigma_{11} = \sigma$, $\sigma_{22} = 0$ and $\sigma_{12} = 0$; for 45º laminates; $\sigma_{11} = \sigma_{22} = 0.5\ \sigma$ and $\sigma_{12} = 0.5\ \sigma$. Since the fibers of the 45º laminates are subjected to a stress level that is half of that acting on the 0º fibers, and the matrix of the former laminates is subjected to shear stress (σ_{12}) while that of the latter is not; therefore, the 45º laminates failure would be matrix dominated compared to the 0º laminates (since the matrix is much weaker than the fibers). In addition, 50% of the fibers in the 0º laminates are aligned with load. This explains why the 0º laminates have higher load carrying capacity compared to the 45º laminate.

$$\begin{bmatrix}\sigma_{11}\\ \sigma_{22}\\ \sigma_{12}\end{bmatrix}=\begin{bmatrix}m^2 & n^2 & 2mn\\ n^2 & m^2 & -2mn\\ -mn & mn & m^2-n^2\end{bmatrix}\begin{bmatrix}\sigma_X\\ \sigma_Y\\ \sigma_{XY}\end{bmatrix} \quad (1)$$

where $m = \cos\theta$ and $n = \sin\theta$, θ is the angle between global (X-Y) and local (1-2) coordinate systems, as shown in Fig. 6.

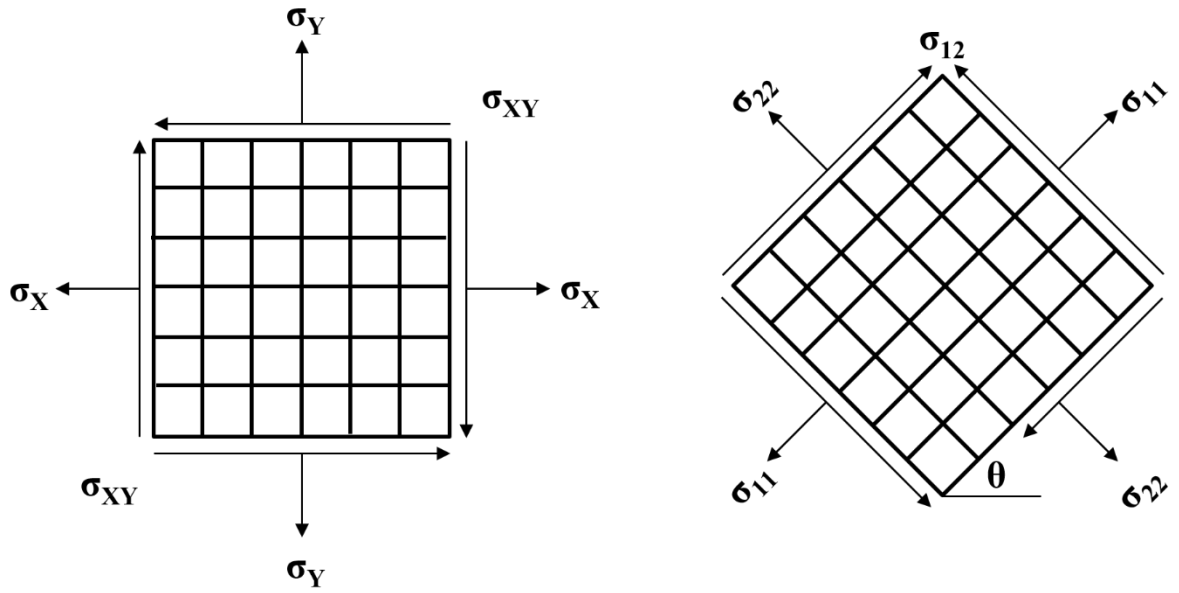

Fig. 6 Stress transformation (local and global coordinates)

In an effort to evaluate the stress concentration effects of the central hole, the ratio of load carrying capacities (F_{max}) were calculated and presented in Fig. 5. In FRP composites, stress concentration effects are function of laminate anisotropy, hole size, stacking sequence and microstructural materials properties (matrix toughness, matrix stiffness and fiber to matrix adhesion) [27]. As shown in Fig. 5, the ratio between F_{max} of sample W/O-Hole and O-Hole 0º and 45º laminates are 1.6 and 1.2, respectively. At the same time, the ratio between the load-carrying area of sample W/O-Hole and O-Hole laminates is 1.2. Therefore, the equivalent stress concentration factor (K_T) for 0º and 45º laminates are 1.3 and 1.0, respectively. In other words, the stress concentration effects in the 45º laminates is negligible.

The current results are supported by the well-known relation for a plate with central circular hole. Equation (2) presents such a relation for an infinitely wide homogeneous plate [28]:

$$\sigma_\theta=\frac{\sigma}{2}\left[1+\frac{a^2}{r^2}-\left(1+3\frac{a^4}{r^4}\right)\cos(2\theta)\right] \quad (2)$$

where, σ_θ is the stress at an angle (θ) from the loading (σ) direction, a is the radius of the circular hole, and r is the radius of the point of interest from the center of the hole

For the 0º laminates, $\sigma_0 = \sigma_{11} = -\sigma$ and $\sigma_{90} = \sigma_{22} = 3\sigma$; and for the 45º laminates, $\sigma_{45} = \sigma_{11} = \sigma$ and $\sigma_{-45} = \sigma_{22} = \sigma$. Since the local stress state, as mentioned above, for the 0º and 45º laminates are ($\sigma_{11} = \sigma$, $\sigma_{22} = 0$ and $\sigma_{12} = 0$) and ($\sigma_{11} = \sigma_{22} = 0.5\,\sigma$ and $\sigma_{12} = 0.5\,\sigma$), respectively. Therefore, the 0º laminates are subjected to local uniaxial loading; however, the 45º laminates are subjected to local biaxial loading. Using the principle of superposition for biaxial loading, the maximum stress (σ_{max}) for the 45º laminates would be equal to the nominal stress (σ). In addition, it has been previously shown that 0º laminates experience the highest stress concentration effects [29].

Figure 7 compares the initial stiffness (before failure onset) of different laminates. It is obvious that the 0º laminates have significantly higher stiffness compared to the 45º laminates; this applies to both the O-Hole and sample W/O-Hole laminates. The O-Hole and sample W/O-Hole samples had almost the same stiffness; i.e., the central hole had insignificant effect on sample initial stiffness. The reason the 0º laminates had higher stiffness compared to the 45º laminates could be explained in terms of local versus global stiffness components, similar to the local stress analysis comparison presented earlier. The insignificant effect for the hole on sample stiffness, for both fiber orientations, could be attributed to the fact that the hole has a more of a localized effect rather than a global effect.

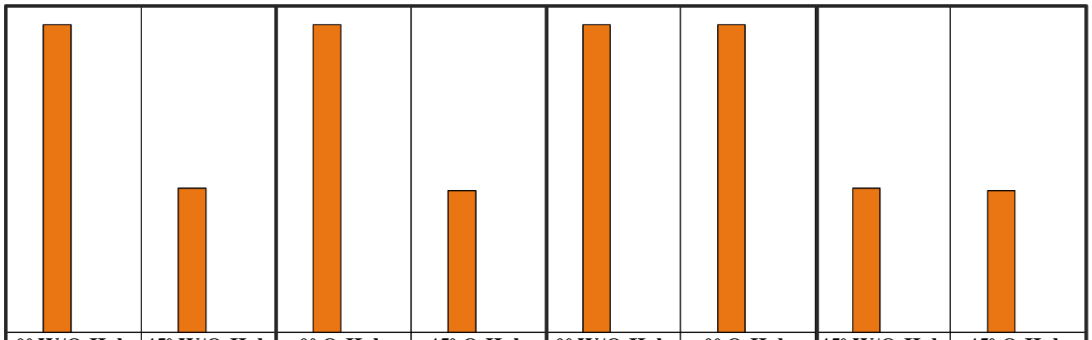

	0º W/O-Hole	45º W/O-Hole	0º O-Hole	45º O-Hole	0º W/O-Hole	0º O-Hole	45º W/O-Hole	45º O-Hole
k [N/m]	1.13E+07	5.30E+06	1.13E+07	5.20E+06	1.13E+07	1.13E+07	5.30E+06	5.20E+06
Ratios	2.1	1	2.2	1	1	1	1	1

Fig. 7 Initial stiffness (before failure onset) of different laminates

Comparing the current predicted results to previously published experimental results, for other FRP materials, show the same trend. Banakar et al. [30] tested 0º and 45º woven glass fiber/epoxy laminates (sample W/O-Hole) under tensile loading. They found that the 0º laminates had almost double the load carrying capacity of the 45º laminates. In addition, the stiffness of the 0º laminates was almost three times that of the 45º laminates. Similar results were also found by Bakir et al. [31] for the same material (glass fiber/epoxy).

3.3 Progressive Failure Analysis of $[0]_4$ Laminates

Figure 8 elaborates the stiffness degradation occurring as the 0º laminates progress towards failure. At the same time, Fig. 9 shows the different stages of progressive failure, in terms of the state variable SDV1. The load-displacement curve (Fig. 8) was divided into three regions, with three different stiffness values. The first region has a stiffness of 11.3 kN/mm, and covers the load-displacement till the first localized fiber failure occurs. The first localized fiber failure occurred at load of about 57% F_{max}, and corresponds to state (2) in Fig. 9. It is important to note that, the first localized matrix failure occurred at about 30% F_{max} (i.e., before the first fiber failure); however, it was not severe enough to cause significant drop in overall stiffness especially that it was very localized, as can been seen from state (1) in Fig. 9. Also, since the first matrix failure was within the fill-tows, and since the warp tows are the principle load carrying constituent, this even made such failure even less significant. However, at 57% F_{max} the composite laminate experienced a matrix constituent failure within the fill-tows in addition to the failure of matrix and fiber within warp-tows, as shown by state (2) in Fig. 9.

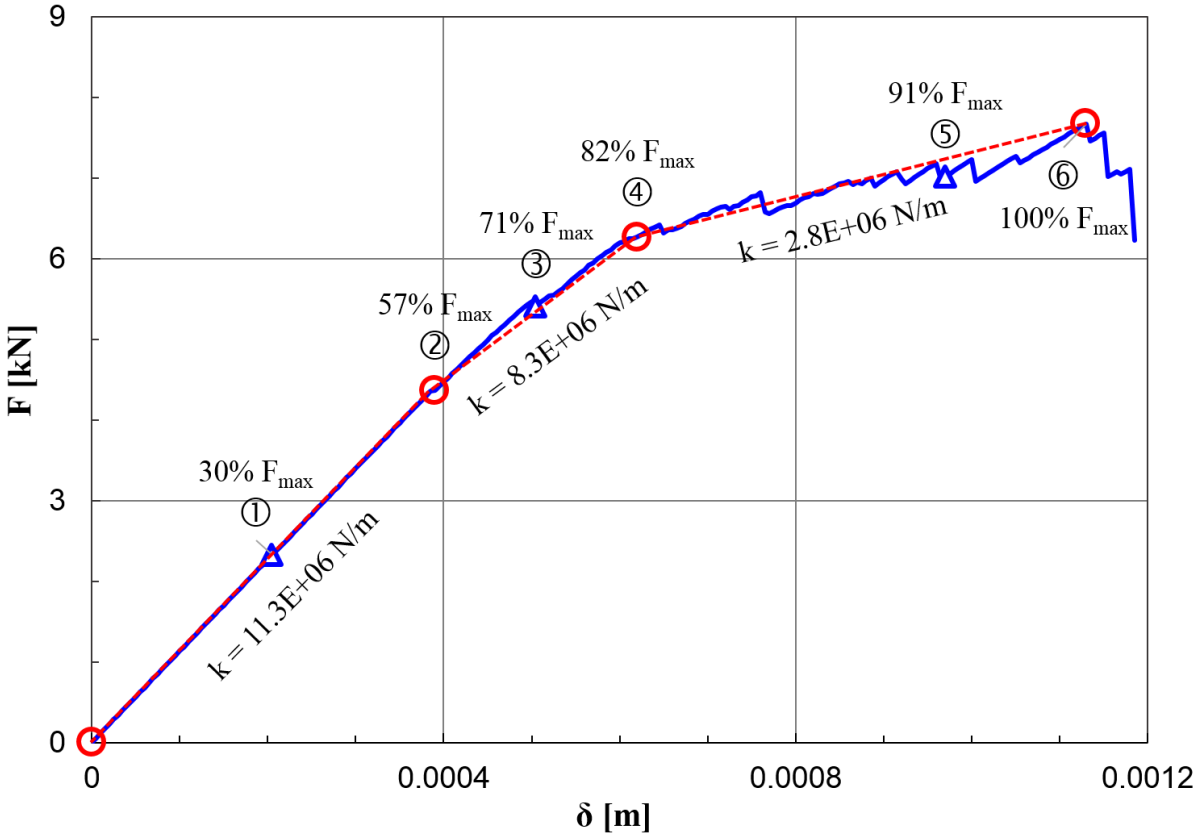

Fig. 8 Load-displacement curve of open-hole $[0]_4$ woven composite laminates

The second region has a stiffness of 8.3 kN/mm, and covers the load-displacement from 57% F_{max} (first localized fiber failure) to about 82% F_{max}. At this level, there is a significant damage increase in the fill matrix pockets, warp matrix pockets and fiber tows at the edge of the hole across the composite laminates. This is when the first significant failure occurred across the whole sample width, and corresponds to state (4) in Fig. 9. It is important to note that, such failure did not represent full failure yet. The third region has a stiffness of 2.8 kN/mm, and covers the rest of the load-displacement till complete failure, where the composite laminate is no longer able to carry any load. This corresponds to state (6) in Fig. 9.

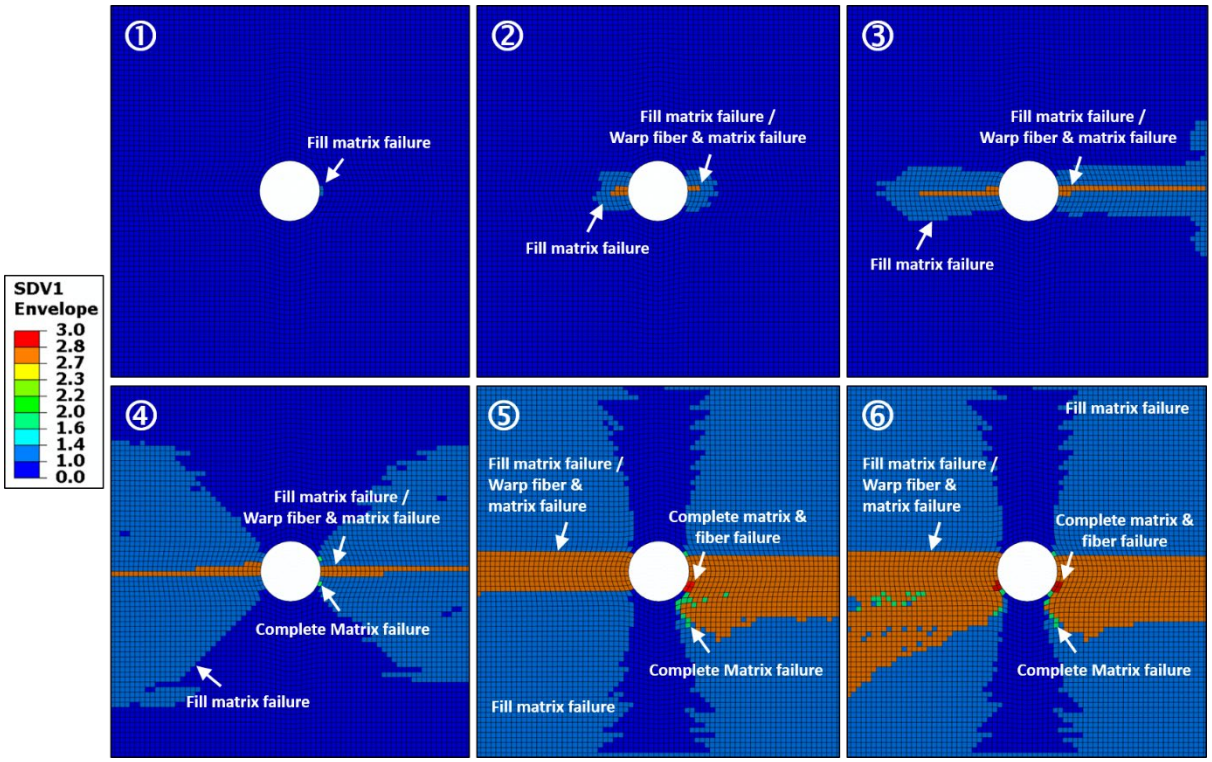

Fig. 9 Progressive failure of open-hole $[0]_4$ woven composite laminates (SDV1 shown)

3.4 Progressive Failure Analysis of $[45]_4$ Laminates

Unlike the 0º laminates, the load-displacement curve of the 45º laminates was divided into only two regions (instead of three), as shown in Fig. 10. Figure 11 presents the corresponding progressive failure states in terms of SDV1.

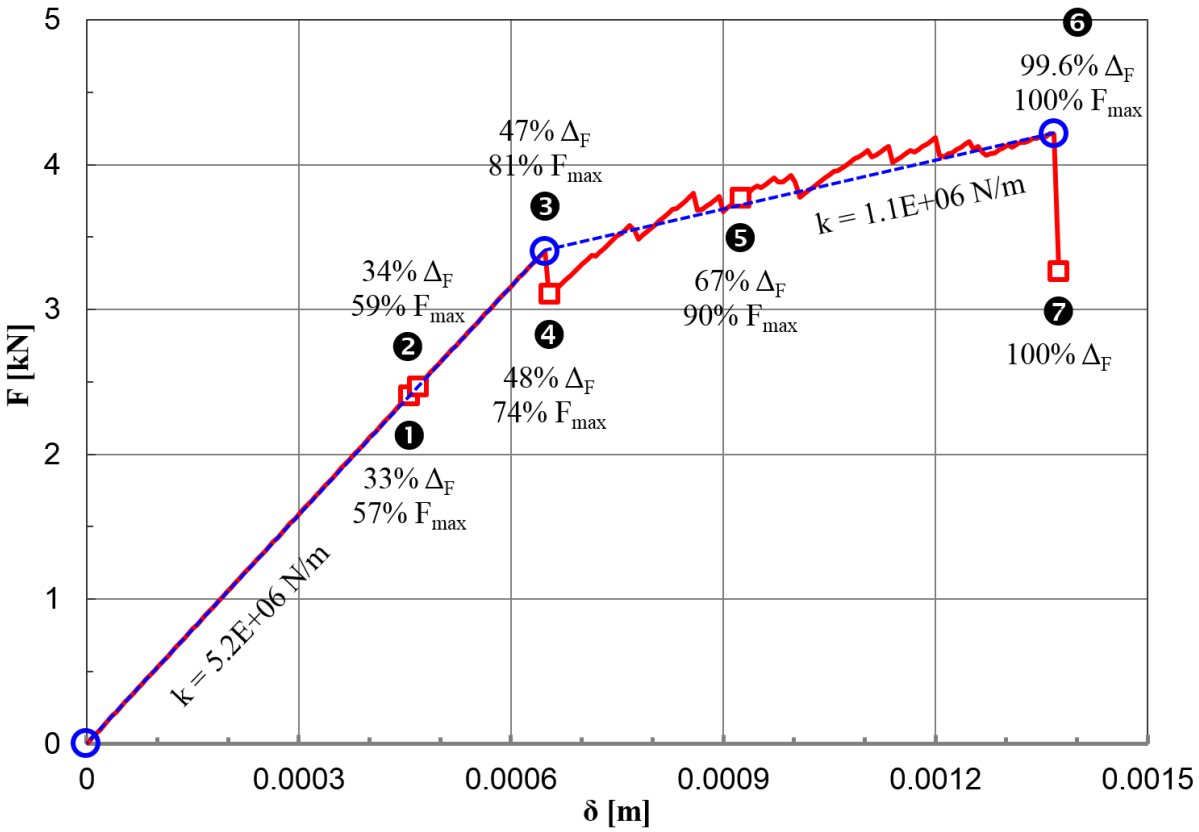

Fig. 10 Load-displacement curve of open-hole $[45]_4$ woven composite laminates

The overall response of the structure appears to be linear up to about 81% F_{max}, where the first significant drop in stiffness is noticed and corresponds to state (3) in Fig. 11. This first region has a stiffness of 5.2 kN/mm. Even though the first localized matrix failure occurred at about 57% F_{max} and the first localized fiber failure occurred at about 74% F_{max}, these failures were not sufficient to produce a significant change in the composite overall stiffness. This is supported by the fact that these failures were much localized, as shown by states (1) & (2) in Fig. 11. It is important to note that, failure is guided by fiber directions (±45º) as was also the case of 0º laminates (0º and 90º). As loading continues, failure progresses, guided by fiber directions and as shown by states (4 - 6) in Fig. 11, till complete failure occurs. At this level, there is sharp drop in stiffness and the composite laminate is no longer capable of carrying any further load.

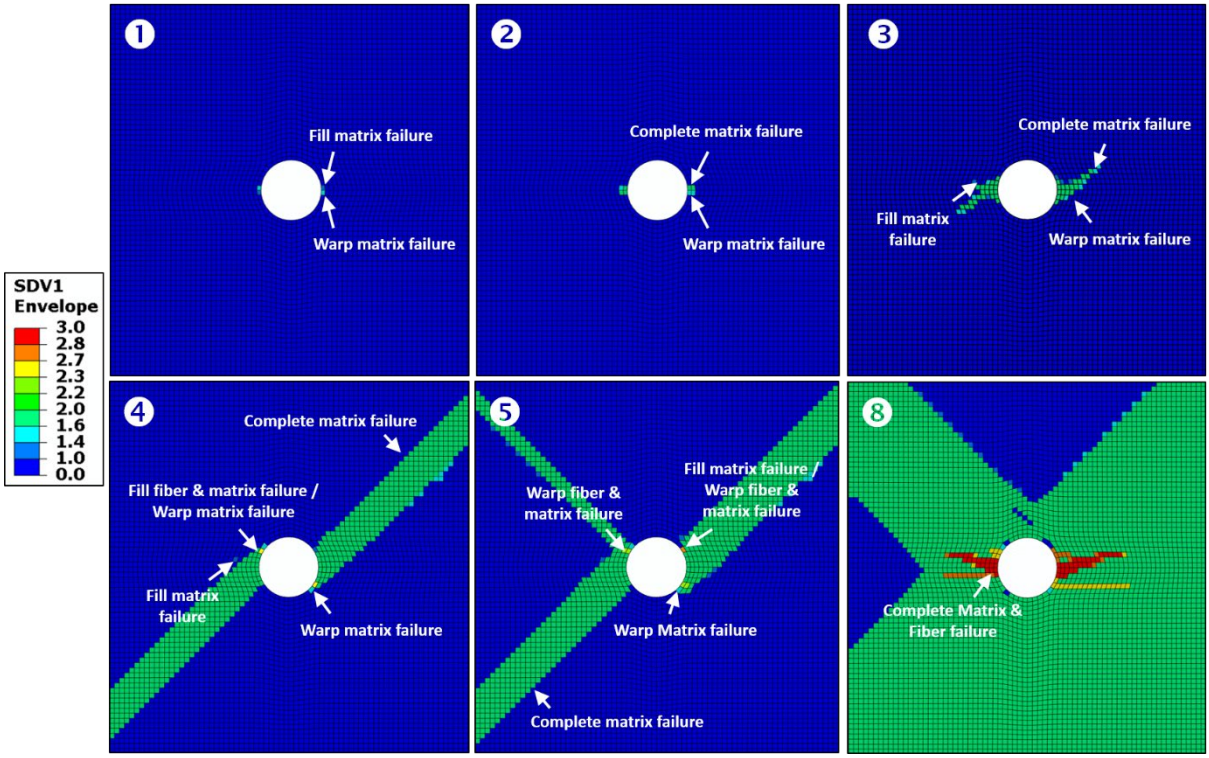

Fig. 11 Progressive failure of open-hole [±45] woven composite laminates (SDV1 shown)

2.3 Conclusion

Based on the current results and discussion, it is concluded that a three dimensional finite element model has been successfully developed, with the aid of multicontinuum theory (MCT), to model progressive failure of plain woven FRP. Woven $[0]_4$ open-hole laminates have higher tensile load carrying capacity, as well as global stiffness, compared to $[45]_4$ laminates. This has been explained in terms of local stress components, and agrees with previously published experimental data. Same conclusion applies to sample without hole laminates. The presence of a central hole has no significant effect on the stiffness of woven composite laminates, for both 0º and 45º orientations. This has been attributed to the much localized effects of the hole, which do not extend to affect the overall sample stiffness. A central hole in a $[0]_4$ woven composite laminate under tensile loading acts as a significant stress raiser; i.e., similar to homogenous materials. However, it has almost an insignificant effect on the maximum stress of $[45]_4$ woven laminates. This has been attributed to the biaxial loading status of the $[45]_4$ laminates compared to the uniaxial status of the $[0]_4$ laminates.

Acknowledgements

The authors would like to thank the Ministry of Higher Education (MOHE) – Egypt for their financial support for performing the current research. Also, they would like to thank the Japan International Cooperation Agency (JICA) for their continuous support to the Egypt-Japan University of Science and Technology (E-JUST).

References

[1] Zebdi O, Boukhili R, Trochu F. An Inverse Approach Based on Laminate Theory to Calculate the Mechanical Properties of Braided Composites. J Reinf Plast Compos 2008;28:2911–30. doi:10.1177/0731684408094063.

[2] Zebdi O. Mechanical Characterization of Braided Composites and Application to Helical Springs. Polytechnic School of Montreal, Montre´ al, QC, Canada, 2004.

[3] Charlebois KM. Evaluation of the Physical and Mechanical Properties of Braided Fabrics and their Composites. J Reinf Plast Compos 2005;24:1539–54. doi:10.1177/0731684405050391.

[4] Carey J, Munro M, Fahim A. Regression-based model for elastic constants of 2D braided/woven open mesh angle-ply composites. Polym Compos 2005;26:152–64. doi:10.1002/pc.20092.

[5] Carey J, Munro M, Fahim A. Longitudinal Elastic Modulus Prediction of a 2-D Braided Fiber Composite. J Reinf Plast Compos 2003;22:813–31. doi:10.1177/0731684403022009003.

[6] Huang Z ming. The mechanical properties of composites reinforced with woven and braided fabrics. Compos Sci Technol 2000;60:479–98. doi:10.1016/S0266-3538(99)00148-7.

[7] Naik NK, Ganesh VK. An analytical method for plain weave fabric composites. Composites 1995;26:281–9.

doi:10.1016/0010-4361(95)93671-6.
[8] Naik RA. Failure Analysis of Woven and Braided Fabric Reinforced Composites. J Compos Mater 1995;29:2334–63. doi:10.1177/002199839502901706.
[9] Ng S-P, Tse P-C, Lau K-J. Numerical and experimental determination of in-plane elastic properties of 2/2 twill weave fabric composites. Compos Part B Eng 1998;29:735–44. doi:10.1016/S1359-8368(98)00025-0.
[10] Lee CS. Virtual Material Characterization of 3D Orthogonal Woven Composite Materials by Large-scale Computing. J Compos Mater 2005;39:851–63. doi:10.1177/0021998305048160.
[11] Tabiei A, Yi W. Comparative study of predictive methods for woven fabric composite elastic properties. Compos Struct 2002;58:149–64. doi:10.1016/S0263-8223(02)00028-4.
[12] Chun H-J, Shin J-Y, Daniel IM. Effects of material and geometric nonlinearities on the tensile and compressive behavior of composite materials with fiber waviness. Compos Sci Technol 2001;61:125–34. doi:10.1016/S0266-3538(00)00201-3.
[13] Belingardi G, Koricho EG, Beyene AT. Characterization and damage analysis of notched cross-ply and angle-ply fabric GFRP composite material. Compos Struct 2013;102:237–49. doi:10.1016/j.compstruct.2013.03.006.
[14] Belmonte HM., Manger CI., Ogin S., Smith P., Lewin R. Characterisation and modelling of the notched tensile fracture of woven quasi-isotropic GFRP laminates. Compos Sci Technol 2001;61:585–97. doi:10.1016/S0266-3538(00)00238-4.
[15] O'Higgins RM, McCarthy MA, McCarthy CT. Comparison of open hole tension characteristics of high strength glass and carbon fibre-reinforced composite materials. Compos Sci Technol 2008;68:2770–8. doi:10.1016/j.compscitech.2008.06.003.
[16] Key C. A three-constituent multicontinuum theory for woven fabric composite materials. Compos Sci Technol 2003;63:1857–64. doi:10.1016/S0266-3538(03)00169-6.
[17] Shindo Y, Watanabe S, Takeda T, Narita F, Matsuda T, Yamaki S. Numerical and experimental evaluation of cryogenic tensile strength of woven fabric-reinforced glass/epoxy composites using open hole specimens. J Mech Mater Struct 2011;6:545–56. doi:10.2140/jomms.2011.6.545.
[18] Clarke JL. Structural Design of Polymer Composites: Eurocomp Design Code and Background Document. CRC Press; 2003.
[19] S-2 Glass Fiber. 15-PL-16154, 1990.
[20] Materials Selector. 1991.
[21] LIGHTER, STRONGER, MORE EFFICIENT DESIGNS 2014. http://www.firehole.com/documents/mct_flyer.pdf.
[22] Hill R. Elastic properties of reinforced solids: Some theoretical principles. J Mech Phys Solids 1963;11:357–72. doi:10.1016/0022-5096(63)90036-X.
[23] Welsh JS, Mayes JS, Biskner AC. EXPERIMENTAL AND NUMERICAL FAILURE PREDICTIONS OF BIAXIALLY-LOADED QUASI-ISOTROPIC CARBON COMPOSITES. 16TH Int. Conf. Compos. Mater., Kyoto, Japan: Kyoto International Conference Center; 2007, p. 1–10.
[24] Key CT, Schumacher SC, Hansen AC. Progressive failure modeling of woven fabric composite materials using multicontinuum theory. Compos Part B Eng 2007;38:247–57. doi:10.1016/j.compositesb.2006.03.006.
[25] Helius MCT 3.0 Tech Brief 2014. http://www.deskeng.com/pics/pdfs/HeliusMCT3TechBrief.pdf.
[26] Garnich MR, Akula VMK. Review of Degradation Models for Progressive Failure Analysis of Fiber Reinforced Polymer Composites. Appl Mech Rev 2009;62:010801. doi:10.1115/1.3013822.
[27] Tensile Testing, 2nd Edition. ASM International; 2004.
[28] Young W, Budynas R. Roark's Formulas for Stress and Strain. McGraw Hill Professional; 2001.
[29] Mallick PK. Fiber-Reinforced Composites: Materials, Manufacturing, and Design, Second Edition. CRC Press; 1993.
[30] Banakar P, Shivananda HK, Niranjan HB. Influence of Fiber Orientation and Thickness on Tensile Properties of Laminated Polymer Composites. Int J Pure Appl Sci Technol 2012;9:61–8.
[31] Yahaya R, Sapuan SM, Jawaid M, Leman Z, Zainudin ES. Effect of fibre orientations on the mechanical properties of kenaf–aramid hybrid composites for spall-liner application. Def Technol 2015. doi:10.1016/j.dt.2015.08.005.